

Investigation of Ge/P-Doped Silica Optical Fibers for Radiation Sensing

K. Kandemir¹, E. Tagkoudi¹, D. Di Francesca¹, and D. Ricci¹

Abstract—The distributed optical fiber radiation sensor (DOFRS) developed by CERN is a key technology for the spatially continuous and real-time monitoring of radiation dose in harsh environments. Silica-based optical fibers (OFs) doped or co-doped with phosphorous are used as sensing elements of the DOFRS systems. The performance of these systems is strongly dependent on the radiation sensitivity of the OFs used, as well as the possibility to qualify and calibrate them for dosimetry applications. In this article, we report on the radiation response of a set of 12 Ge/P-doped single-mode (SM) OFs at 1550 and 1625 nm under ⁶⁰Co γ -rays, including a post-irradiation study to evaluate the recovery of the fibers under test. After conducting several experiments to evaluate the performance of the OFs, we determined which ones are the most suitable to be used in the radiation sensing fiber optics cables installed in CERN's accelerator complex.

Index Terms—Color centers, distributed fiber sensors, dosimetry, Ge-doped, optical fibers (OFs), P-doped, radiation effects, radiation-induced attenuation (RIA), γ -rays.

I. INTRODUCTION

CERN, the European Organization for Nuclear Research, is a world-leading research institution in the field of high-energy physics research. One of the challenges of working with high-energy particle accelerators and detectors is the necessity for monitoring the ionizing radiation levels accurately and reliably for ensuring the safety of personnel and the protection of sensitive equipment against potential damage or malfunction and failure. The distributed optical fiber radiation sensor (DOFRS) system has emerged as a very well-adapted technological innovation to meet this goal [1], [2], [3]. Specifically designed to operate within CERN's accelerator complex, the DOFRS system provides a solution for monitoring radiation dose levels in the mixed-field environment of CERN. It presents some complementary features over traditional dosimeters [4], [5], [6], [7]. It enables distributed measurements with 1-m level spatial resolution and potentially covering kilometer-scale distances. Furthermore, it allows real-time and online monitoring while preserving the key benefits shared with other optical fiber (OF)-based

sensors such as the compact size, flexibility, and immunity to electromagnetic interference [8], [9], [10].

The working principle of a DOFRS system is based on the phenomenon known as radiation-induced attenuation (RIA). RIA occurs in OFs that are exposed to ionizing radiation, a prevalent environmental condition in particle accelerators, nuclear power plants, nuclear waste repositories, and space.

Upon exposure to ionizing radiation, point defects are created in the OF core and cladding materials. These radiation-induced defects absorb light propagating in the OF and, as a result, they are largely responsible for the appearance of the RIA [11], [12], [13]. RIA is a cumulative effect strongly influenced by various parameters, including the total radiation dose, the specific composition, and the fabrication method of the OF. The dose rate, the type of radiation, and the irradiation temperature constitute additional parameters influencing the RIA.

It is important to note that most of the OFs are not suitable for dosimetry applications. Standard OFs, primarily used for telecommunications, lack the necessary properties to effectively function as reliable dosimeters [9]. Fiber dosimetry typically requires specific doping and manufacturing procedures. The selection of the appropriate OF for dosimetry applications is a crucial factor for ensuring accurate measurements. The key characteristics of a good RIA-based fiber are a strictly monotonic RIA dependence on the dose, the absence of spontaneous recovery after the end of irradiation, the lack of dose rate dependence on the RIA, and the absence of photo-bleaching effects induced by the injected light [9].

While P-doped OFs have been already proven to be excellent candidates for fiber dosimetry [9], [14], [15], Ge/P-doped OFs have exhibited promising yet preliminary results in the domain of radiation sensing and their capabilities in fiber sensing need to be further explored [16], [17], [18], [19]. The utilization of DOFRS systems requires different OF sensors, each one possessing different sensitivities, to effectively monitor environments with a wide spectrum of radiation levels. The P-doped OF exploited and reported in [9] is suitable for detecting radiation dose levels starting at approximately 1 Gy(SiO₂).

The aim of the study was to investigate the behavior of Ge/P-doped OFs under irradiation and evaluate their suitability for integration and use within DOFRS systems. This exploitation has been performed at two wavelengths 1550 and 1625 nm. Moreover, some spectral measurements and sensitivity calculations are also reported. The investigation

Manuscript received 20 March 2024; revised 3 April 2024; accepted 25 April 2024. Date of publication 29 April 2024; date of current version 16 August 2024. (K. Kandemir and E. Tagkoudi contributed equally to this work.) (Corresponding author: D. Di Francesca.)

The authors are with the European Organization for Nuclear Research (CERN), CH-1211 Geneva, Switzerland (e-mail: eirini.tagkoudi@cern.ch; diego.di.francesca@cern.ch).

Color versions of one or more figures in this article are available at <https://doi.org/10.1109/TNS.2024.3394879>.

Digital Object Identifier 10.1109/TNS.2024.3394879

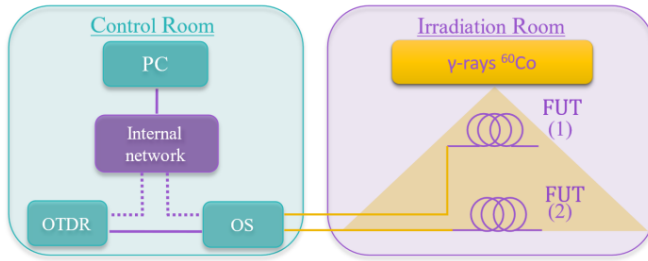


Fig. 1. Schematic representation of the experimental setup. OTDR: optical time-domain reflectometer. OS: optical switch. position (1) corresponds to a dose rate 41.26 Gy/h and position (2) corresponds to a dose rate of 2.35 Gy/h.

and analysis allowed us to select one of the Ge/P-doped OFs for the following in-depth study. Subsequently, the same OF was the selected one for the manufacturing of the OF cable, which has been installed at CERN’s accelerator complex during the Long Shutdown 2.

II. EXPERIMENTAL DETAILS

We experimentally investigated 12 single-mode (SM) OFs using a CERN ^{60}Co irradiation facility. The 12 OFs under study are commercial Ge/P doped OFs that respect the ITU-T G.652.D standard and that are nominally identical. They all originate from a single production line and production process. They have been selected for investigation after a first study led by CERN which is reported in [17], which allowed to identify a supplier capable of such production. The ^{60}Co facility is primarily utilized for qualification tests of electronic components and for examining the effects of total ionizing dose (TID). It consists of a control room and an adjacent irradiation room, as shown in Fig. 1. For this experiment, the two rooms were connected through radiation-resistant OF links. To achieve different dose rates, the relative distances between the ^{60}Co source and the samples were adjusted.

Before each experiment, we measured the dose rate at each position using an ionization chamber. The uncertainty on the dose rate is 5% at 2σ and all reported doses are in SiO_2 .

To measure the RIA, we used the experimental setup of Fig. 1. It consists of an optical time-domain reflectometer (OTDR) MTS-6000A from VIAVI Solutions coupled with an optical switch (OS) MAP-2000 from the same supplier. There are two reasons for this choice. The first one is that it gives the possibility to test several samples in parallel in the same irradiation conditions, which is a preferable configuration in comparative RIA studies. The second reason is that such a setup is used in real implementations of the DOFRS system. In general, when testing OF for dosimetry, it is preferable that the test conditions are as close as possible to the actual operational conditions. This is especially important to ensure that photobleaching effects are under control.

We coiled up 15-m-long OF samples in spools of different diameters (>6 cm) and connected them to different channels of the OS. All samples were mounted behind and in contact with 4-mm-thick acrylic plate to reach radiation equilibrium. Each sample was extracted from a different spool, and it is possible that all different spools originated from different OF preforms. In the following, we are using the naming

convention “Ge/P_n” for the Ge/P-doped fiber samples, where n is the number that identifies the spool of origin.

All tests were conducted at room temperature and the electronic devices were placed in the control room to prevent them from being exposed to radiation. The integration time of each single OTDR trace was set to 1 min and the pulse duration to 2 ns to obtain a spatial resolution of approximately 0.5 m.

III. EXPERIMENTAL RESULTS

In this section, we present the experimental results of the RIA response of 12 SM Ge/P-doped OFs exposed to γ -ray irradiation. We carried out three separate experiments, which will be detailed in the upcoming subsections. The first experiment was a screening of the 12 OFs at one dose rate, the second experiment was the selection of some OFs for further study at two different dose rates, while in the third experiment, we only focus on the irradiation and post-irradiation behavior of a single OF.

A. First Irradiation Test of 12 Different Ge/P-Doped OFs

In the first experiment under γ -rays, we used a dose rate of 41.26 Gy/h for all 12 OF samples and irradiated them up to 100 Gy during three irradiation runs. This test was primarily conducted to evaluate the sensitivity in such conditions as well as the possible recovery of all OFs. After reaching the 100-Gy dose, we monitored the post-irradiation behavior online for a period of 17.5 h.

Fig. 2(a) illustrates the RIA growth as a function of the time of the 12 fiber samples at a wavelength of 1550 nm at room temperature. Fig. 2 shows that there was a significant difference in their RIA response under irradiation as well as in their post-irradiation behavior.

The behavior of the OFs in the magenta and cyan groups appeared to be the most promising for their application as radiation dosimeters. These two groups were chosen to undergo a new set of experiments for further investigation of their RIA response under higher doses and different dose rates.

B. Second Irradiation Test of Six Selected OFs

After performing the initial irradiation tests on all available samples, six of them were used for further testing: Ge/P_01, Ge/P_02, Ge/P_06, Ge/P_10, Ge/P_11, and Ge/P_12. These selected fibers underwent more detailed measurements at two different dose rates, 41.26 Gy/h and 2.35 Gy/h (Fig. 1), and significantly higher radiation doses.

Fig. 3 shows the response of the RIA of the six OFs as a function of the TID for the two dose rates. As depicted in Fig. 3(a), the fibers were irradiated up to ~ 8 kGy for the tests conducted at a dose rate of 41.26 Gy/h and up to ~ 450 Gy for the tests at 2.35 Gy/h, as shown in Fig. 3(b).

Fig. 4 illustrates the fiber sensitivity—in dB/m/Gy—of the six OFs under investigation, calculated based on the linear part of the irradiation response curves presented in Fig. 3. The sensitivities are estimated for both measured wavelengths of 1550 nm [Fig. 4(a)] and 1625 nm [Fig. 4(b)]. More precisely, the fiber sensitivity is calculated within a range of up to 500 Gy

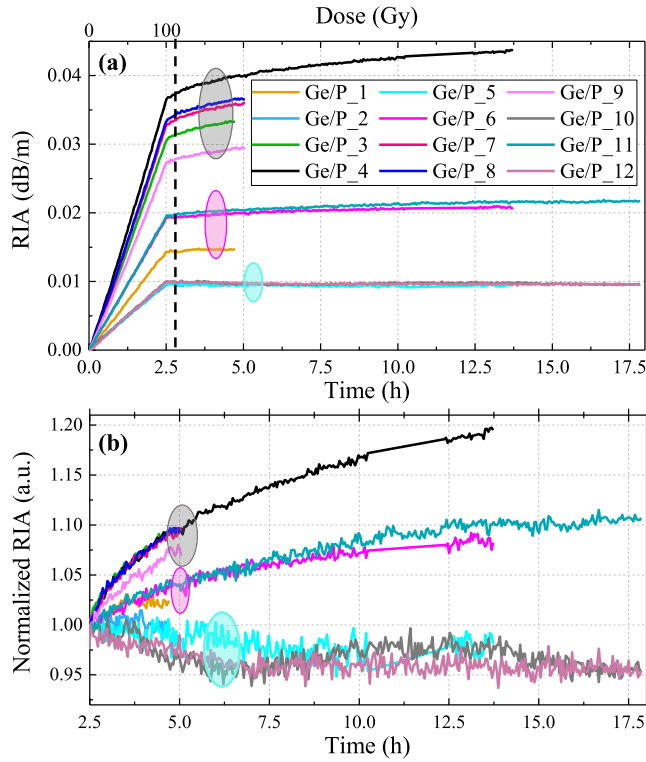


Fig. 2. (a) RIA evolution as a function of the time at room temperature for the 12 investigated OFs at 1550 nm for a dose rate of 41.26 Gy/h. The stop of the irradiation is indicated at 100 Gy with a black dashed line. (b) Normalized RIA as a function of time after the stop of the irradiation.

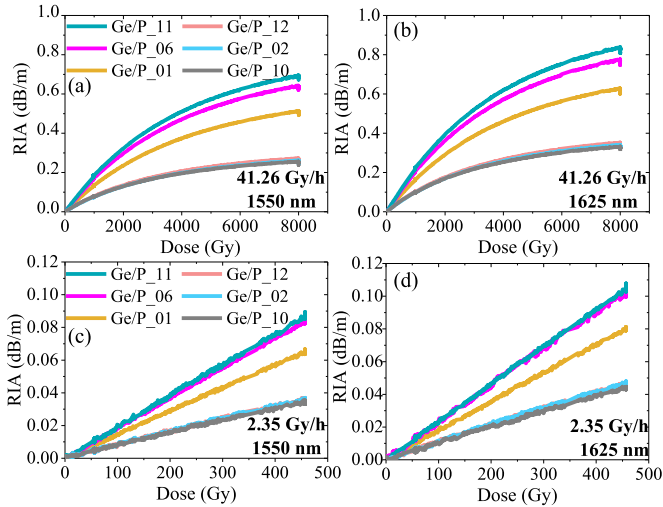


Fig. 3. RIA as a function of the total accumulated dose at room temperature for the six OFs under study measured at (a) wavelength of 1550 nm and (b) wavelength of 1625 nm at a dose rate of 41.26 Gy/h, and (c) at 1550 nm and (d) 1625 nm at a dose rate of 2.35 Gy/h.

for the highest dose rate of 41.26 Gy/h. Conversely, for the lowest dose rate of 2.35 Gy/h, we calculated the sensitivity from up to 55 Gy for both investigated wavelengths.

We observe a ~ 1.3 times higher sensitivity at 1625 nm [Fig. 4(b)] across all six chosen OFs when compared to sensitivities at 1550 nm [Fig. 4(a)].

Following the irradiation tests of the selected six OFs, we decided to further investigate the irradiated Ge/P-doped

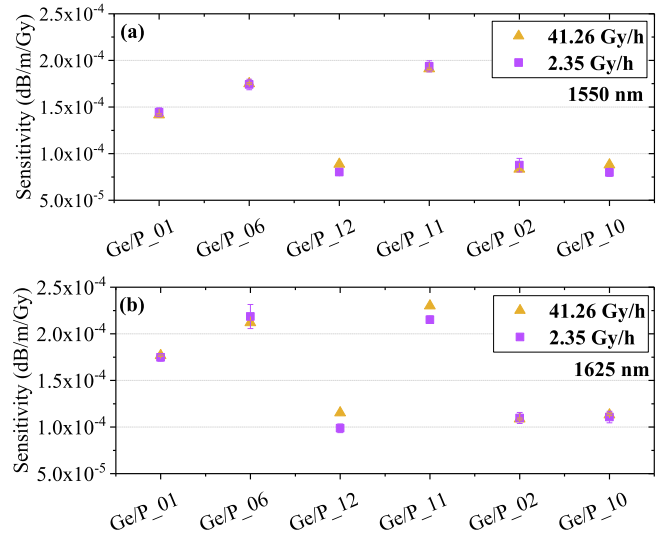


Fig. 4. Sensitivity—in dB/m/Gy—for the six selected OFs at (a) 1550 nm and (b) 1625 nm for the two different dose rates of 41.26 Gy/h (yellow) and 2.35 Gy/h (purple).

samples by performing postmortem spectral measurements utilizing the cutback technique, which is a standard method to determine the optical attenuation of an OF.

The experimental setup for performing cutback measurements consists of a very stable halogen light source and a near-infrared spectrometer. Initially, a measurement of the transmitted light spectrum is performed in a long OF sample, and subsequently, a portion of the same sample is carefully cut, leading to a shorter length of OF sample.

Although the spectrometer is capable of recording spectra from 900 nm up to $1.7 \mu\text{m}$, only the part above the cutoff wavelength, at about $1.2 \mu\text{m}$, can be reproduced reliably and it is reported here.

Fig. 5 shows the RIA of the six irradiated OFs as a function of wavelength for the samples irradiated at a dose rate of 2.35 Gy/h up to 450 Gy [Fig. 5(a)] and 41.26 Gy/h up to 8 kGy [Fig. 5(b)]. The wavelength dependence is such that higher RIA values are measured at longer wavelengths. RIA reaches the values of 0.15 dB/m at $1.7 \mu\text{m}$ for an irradiation up to 8 kGy and 0.8 dB/m at $1.7 \mu\text{m}$ for an irradiation up to 450 Gy.

C. Third Irradiation Test of One Selected OF

Among the six fibers examined in the previous set of experiments, we selected Ge/P_06 for further investigation and post-irradiation monitoring. It exhibited similar behavior with the Ge/P_11 according to Figs. 2 and 3 and also similar radiation sensitivity to the fiber investigated in [17]. The objective of this irradiation was to reproduce the results of the second test and reach a total dose of at least 10 kGy. The selected OF was exposed to a dose rate of 38.6 Gy/h. The results are compared to the lowest and highest dose rate data, which are derived from the second irradiation experiment discussed in Section III-B. During this irradiation test, the OF was irradiated up to 13 kGy during 14 days of irradiation with 2.5 days of recovery

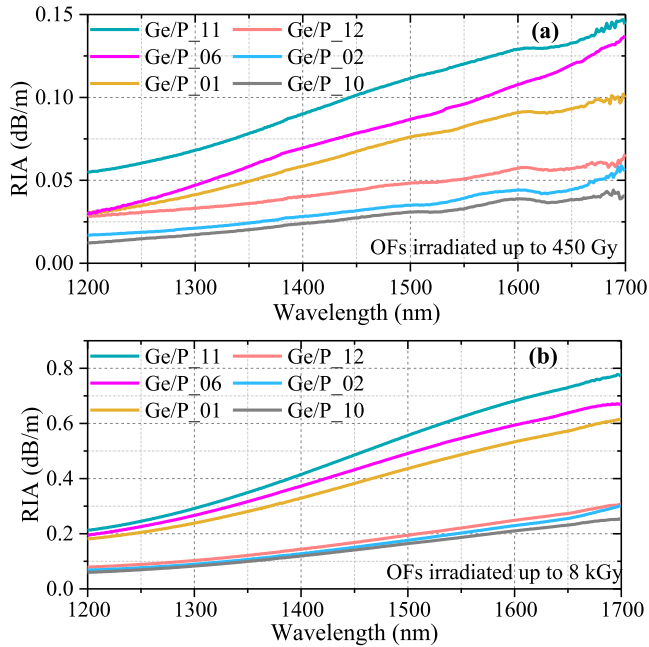


Fig. 5. RIA spectral measurements in part of the SWIR transmission window of the six selected Ge/P-doped OFs irradiated (a) up to 450 Gy with a dose rate of 2.35 Gy/h and (b) up to 8 kGy with a dose rate of 41.26 Gy/h.

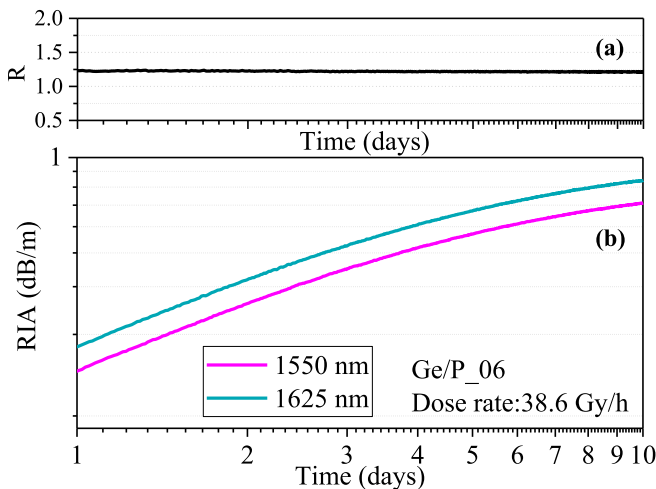


Fig. 6. (a) Ratio (R) between the RIA at 1625 nm and RIA at 1550 nm. (b) Time dependence of the RIA after the end of irradiation at room temperature for one selected fiber Ge/P_06 for a dose rate of 38.6 dB/m at 1550 and 1625 nm.

(post-irradiation period). The Ge/P-doped OFs for this experiment were located in close proximity of position (1) in Fig. 1.

Fig. 6(b) shows the time dependence—in logarithmic scale—of the RIA at room temperature for the two investigated wavelengths of 1550 and 1625 nm at a dose rate of 38.6 Gy/h for the selected Ge/P_06 OF. The ratio between the RIAs at 1550 and 1625 nm $R = (\text{RIA}(\lambda_2 = 1625)/\text{RIA}(\lambda_1 = 1550))$ is plotted in Fig. 6(a). We calculate a near-constant ratio of 1.25, close to the previous irradiation test (Section III-B).

In Fig. 7(a), the RIA as a function of the dose is presented for the investigated wavelength of 1550 nm. In Fig. 7(b), we present the post-irradiation phase after the termination of

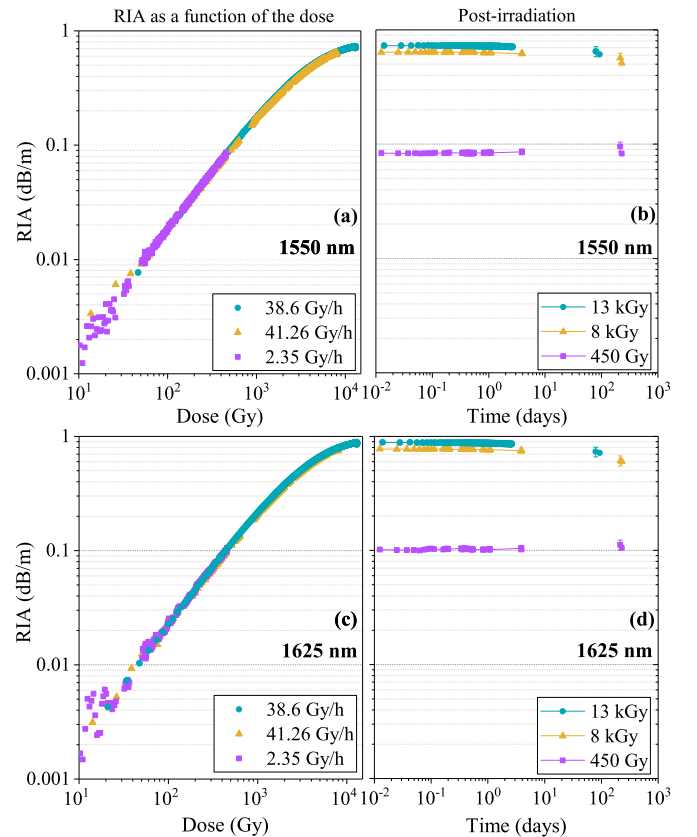


Fig. 7. (a) RIA as a function of dose and (b) recovery over time for the selected Ge/P-doped OF at 1550 nm. (c) RIA as a function of the dose and (d) recovery over time for the selected Ge/P-doped OF at the wavelength of 1625 nm. These are the calibration curves obtained for the three different dose rates: 38.6, 41.26, and 2.35 Gy/h.

the irradiation for the three different dose rates at 1550 nm. Extending the experimental study, Fig. 7(c) and (d) shows the RIA as a function of the dose and the subsequent recovery process of the selected OF at the wavelength of 1625 nm.

The post-irradiation monitoring process consisted of two stages. The first stage was conducted immediately after the irradiation by simply continuing the data acquisition. Long-term monitoring of the losses has been carried out up to 80 days after the stop of the irradiation at 13 kGy and 215 days after the stop of the irradiation at 8 kGy and 450 Gy. During this period, the fibers were always kept at room temperature. In this way, we were able to record the recovery effect over a period comparable to the lifetime of a sensor at CERN. The studied Ge/P fibers did not show a significant recovery over the long post-irradiation period nor a significant dose rate dependence; the overlap of the RIA versus dose curves is satisfactory at both 1550 and 1625 nm.

The sensitivity of the fiber to radiation, measured on a linear scale, is 0.175 dB/km/Gy at the investigated wavelength of 1550 nm.

IV. DISCUSSION

We examined a series of OFs designed for telecommunications and containing Ge and P as doping elements. Since the specific chemical composition of the core and cladding

regions was not disclosed by the supplier, the interpretation of the results relies on certain assumptions. It is noteworthy that fibers conforming to the commercial ITU-T G652.D standard typically exhibit low doping levels, often just a few percent. Given that both Ge and P dopants contribute to an increase in the refractive index, it is reasonable to infer that the OFs under investigation have comparably low doping levels. In addition, previous studies on OFs doped with Ge and P indicate Ge as the primary dopant, with P present at a concentration a few times lower as shown in [20]. It is important to note that P may also function as a co-dopant, appearing exclusively in the cladding region of the fiber. However, when present in the purely Ge-doped core, the concentration of Ge can be significantly higher, approximately 12 wt% as mentioned in [9].

From the experiments presented in Section III-A—related to the first irradiation and OF screening—all OF samples showed a linear dependence of RIA with a dose up to 100 Gy, which was the final dose for the first irradiation. A closer look at Fig. 2(a) and (b) reveals that we can group the 12 fibers into three classes and that the most radiation-sensitive OF is approximately 3.5 times more sensitive than the least radiation-sensitive one. The first group, indicated by the gray circle, contains the Ge/P_n fibers that exhibited an approximately 20% increase in RIA during the post-irradiation period. The second group, indicated by a magenta circle, showed a 10% increase in RIA after the end of the irradiation. Finally, the third group of OFs, indicated by a cyan circle, displayed a 5% decrease in RIA after the termination of irradiation. Another interesting aspect is that the most radiation-sensitive OFs are the ones that exhibited the highest increase of optical attenuation after the irradiation stop.

This phenomenon is quite different from the typical behavior of the majority of standard OFs, which usually undergo a recovery process after the stop of irradiation. A similar but not as strong behavior has been reported in P-doped OFs [9]. Our research seems to indicate that achieving RIA reproducibility is challenging in the sample type we examined, even when ensuring that all fibers and preforms come from the same production line and process. The variation in the radiation response among different OFs is likely due to the fact that the samples are coming from different preforms, which means that their chemical composition and manufacturing processes might have some slight variability, which produces a significant sensitivity change to radiation. This has two important practical implications. First, OFs used in dosimetry applications should undergo at least partial calibration on a spool-by-spool basis, unless high reproducibility of radiation response can be ensured by other means. Second, researchers performing extensive studies on samples extracted from a single spool or very limited number of fiber spools could face difficulties in drawing broad quantitative conclusions about that specific fiber type.

It is evident from the results of Fig. 3 that none of the six selected investigated OFs reached saturation at a total dose of 8 kGy, which makes them very good candidates for radiation monitoring within this range of doses. The maximum value of RIA for the highest accumulated dose was 0.7 dB/m, and as

a result, such OF would be well suited to monitor radiation levels significantly higher than the ones targeted with the P-doped OFs studied in [3].

Our analysis shows that the RIA has a linear response to the accumulated dose up to approximately 1.2 kGy, and thus, a linear fit can be used for the OF calibration within this dose range. However, at about 1.2 kGy, the RIA starts displaying a sublinear dependence on the dose that causes an error on the TID larger than 5%. Therefore, especially for dose levels beyond 1.2 kGy, a full experimental calibration curve is essential to obtain an accurate result of TID measurement and it is not possible to rely on a single calibration coefficient. Upon comparison with the P-doped OFs analyzed in [9], in the range from 0 to 500 Gy, the difference in sensitivity between the P-doped and the Ge/P-doped OF is roughly a factor of 20, which is likely due to a significantly lower P doping in the core and/or cladding region of the Ge/P doped OF. This is a very important result as it evidences the complementarity of the two different OF sensor types in monitoring environments with substantially different radiation levels.

Moreover, the ~1.3 times higher sensitivity at 1625 nm with respect to 1550 nm implies that, for Ge/P co-doped OFs, the specific choice of interrogation wavelength can be exploited to further adjust the sensitivity of the sensor to the radiation environment that needs to be monitored. This characteristic is absent in purely P-doped single-mode OFs that usually show a sensitivity difference of very few percent from 1550 to 1625 nm [9]. Furthermore, it is worth noting that many SM OTDR devices also support an additional standard interrogation wavelength of 1310 nm. In principle, and after experimental validation, a single Ge/P-doped OF could easily provide a third sensitivity at 1310 nm, which according to Fig. 4(a) would be about a factor of 2 lower than the one at 1550 nm. This would be indeed a very versatile solution to address complex radiation environments. As this functionality enhances greatly the practicality and the efficiency of an OF radiation monitor, it will be further explored in future investigations.

Regarding the spectral response of the investigated OF reported in Fig. 5, it is noteworthy that the spectra do not distinctly exhibit the infrared absorption band associated with the P1 defect. This particular defect typically dominates the RIA spectra of P-doped OFs [9]. The P1 defect is characterized by an unpaired electron localized on a threefold coordinated phosphorus atom, and its absorption band usually peaks at around 0.79 eV with a full-width at half-maximum (FWHM) of approximately 0.29 eV [21], [22]. However, several factors may influence the shape of RIA spectra in OFs such as the ones we have investigated. In [23], we have illustrated how differences in the radiation responses between core and cladding materials can lead to modulation in the absorption bands associated with the P1 defect in SM fibers, compared to results obtained from homogeneous bulk samples or MM fibers. This modulation is determined by the confinement factor, specifically the light power propagating inside the core. Expanding on the findings in [9], it can be asserted that a radial distribution of point defects concentrated toward the center of the core could result in an apparent blueshift of

the associated absorption band. Conversely, a concentration of the same defects in the periphery of the core or in the cladding regions could induce a redshift. Based on the spectra presented in Fig. 5, one might lean toward assuming the latter case. At the same time, one should be aware of the potential presence of point defects that absorb light in the NIR region similar to the P1 but that have a different structure also involving the Ge dopant. To the best of our knowledge, such a possibility has not been reported in the literature and deserves further investigation using experimental techniques, such as electron paramagnetic resonance, which could perhaps confirm this hypothesis.

Even if the clear presence of the P1 point defect may not be visually apparent from Fig. 5, the constant ratio between the RIAs at 1550 and 1625 nm (Fig. 6) can be a noteworthy indicator that the RIA is dominated by a single defect type. However, for the sake of rigor, it should be acknowledged that the possibility of multiple point defects coexisting and undergoing concurrent creation and transformation processes in fixed ratios cannot be entirely ruled out.

V. CONCLUSION

We carried out an experimental investigation of 12 SM Ge/P-doped OFs to evaluate their radiation response under ^{60}Co γ -rays. The study includes the post-irradiation behavior of the OFs under test. After the first fiber screening, we narrowed down to six promising fiber samples and eventually selected a single Ge/P-doped fiber for an in-depth study. The study at three different dose rates and the long-term post-irradiation behavior showed the potential of this type of Ge/P-doped OF for radiation monitoring and dosimetry for doses up to a few kGys, significantly higher than what was reported in P-doped OF in [9]. This OF type showed a radiation sensitivity about 20 times lower than the P-doped OF used for DOFRS and reported in the literature. After this investigation, the OF was considered suitable for radiation monitoring and was added to the DOFRS OF cables installed and used in CERN's accelerator complex.

REFERENCES

- [1] H. Henschel, M. Körfer, J. Kuhnenn, U. Weinand, and F. Wulf, "Fibre optic radiation sensor systems for particle accelerators," *Nucl. Instrum. Methods Phys. Res. A, Accel. Spectrom. Detect. Assoc. Equip.*, vol. 526, no. 3, pp. 537–550, Jul. 2004.
- [2] D. Di Francesca et al., "Dosimetry mapping of mixed-field radiation environment through combined distributed optical fiber sensing and FLUKA simulation," *IEEE Trans. Nucl. Sci.*, vol. 66, no. 1, pp. 299–305, Jan. 2019.
- [3] A. H. Hartog, *An Introduction to Distributed Optical Fibre Sensors*, 1st ed. Boca Raton, FL, USA: CRC Press, 2018.
- [4] E. B. Holzer et al., "Beam loss monitoring for LHC machine protection," *Phys. Proc.*, vol. 37, pp. 2055–2062, Jan. 2012.
- [5] G. Spiezia et al., "The LHC radiation monitoring system-RadMon," in *Proc. 10th Int. Conf. Large Scale Appl. Radiat. Hardness Semiconductor Detectors Firenze*, Jul. 2011, pp. 1–12.
- [6] K. Bilko et al., "Radiation environment in the LHC arc sections during run 2 and future HL-LHC operations," *IEEE Trans. Nucl. Sci.*, vol. 67, no. 7, pp. 1682–1690, Jul. 2020.
- [7] K. Bilko et al., "CERN super proton synchrotron radiation environment and related radiation hardness assurance implications," *IEEE Trans. Nucl. Sci.*, vol. 70, no. 8, pp. 1606–1615, Aug. 2023.
- [8] P. Lu et al., "Distributed optical fiber sensing: Review and perspective," *Appl. Phys. Rev.*, vol. 6, no. 4, pp. 1–35, Dec. 2019.
- [9] D. Di Francesca et al., "Qualification and calibration of single-mode phosphosilicate optical fiber for dosimetry at CERN," *J. Lightw. Technol.*, vol. 37, no. 18, pp. 4643–4649, Sep. 15, 2019.
- [10] G. L. Vecchi et al., "Distributed optical fiber radiation sensing at CERN; distributed optical fiber radiation sensing at CERN," in *Proc. 9th Int. Part. Accel. Conf. (IPAC)*, Vancouver, BC, Canada, Apr. 2018, pp. 2039–2042.
- [11] P. Stajanca and K. Krebber, "Radiation-induced attenuation of perfluorinated polymer optical fibers for radiation monitoring," *Sensors*, vol. 17, no. 9, p. 1959, Aug. 2017.
- [12] D. Di Francesca et al., "Radiation-induced attenuation in single-mode phosphosilicate optical fibers for radiation detection," *IEEE Trans. Nucl. Sci.*, vol. 65, no. 1, pp. 126–131, Jan. 2018.
- [13] A. L. Tomashuk, M. V. Grekov, S. A. Vasiliev, and V. V. Svetukhin, "Fiber-optic dosimeter based on radiation-induced attenuation in P-doped fiber: Suppression of post-irradiation fading by using two working wavelengths in visible range," *Opt. Exp.*, vol. 22, no. 14, p. 16778, Jul. 2014.
- [14] A. Morana et al., "Operating temperature range of phosphorous-doped optical fiber dosimeters exploiting infrared radiation-induced attenuation," *IEEE Trans. Nucl. Sci.*, vol. 68, no. 5, pp. 906–912, May 2021.
- [15] D. Di Francesca et al., "Low radiation dose calibration and theoretical model of an optical fiber dosimeter for the international space station," *Appl. Opt.*, vol. 62, no. 16, p. E43, Jun. 2023.
- [16] C. Campanella et al., "Combined temperature and radiation effects on radiation-sensitive single-mode optical fibers," *IEEE Trans. Nucl. Sci.*, vol. 67, no. 7, pp. 1643–1649, Jul. 2020.
- [17] I. Toccafondo, "Distributed optical fiber radiation and temperature sensing at high energy accelerators and experiments," Ph.D. thesis, CERN, Geneva, Switzerland, 2015.
- [18] P. Borgermans et al., "On-line gamma dosimetry with phosphorous and germanium co-doped optical fibres," in *Proc. 5th Eur. Conf. Radiat. Effects Compon. Syst.*, Sep. 1999, pp. M-16–M-19.
- [19] H. Henschel, O. Köhn, and H. U. Schmidt, "Optical fibres as radiation dosimeters," *Nucl. Instrum. Methods Phys. Res. Sect. B, Beam Interact. Mater. At.*, vol. 69, pp. 307–314, Jun. 1992.
- [20] S. Girard, J. Keurinck, Y. Ouerdane, J.-P. Meunier, and A. Boukenter, "Gamma-rays and pulsed X-ray radiation responses of germanosilicate single-mode optical fibers: Influence of cladding codopants," *J. Lightw. Technol.*, vol. 22, no. 8, pp. 1915–1922, Aug. 2004.
- [21] D. L. Griscom, E. J. Friebele, K. J. Long, and J. W. Fleming, "Fundamental defect centers in glass: Electron spin resonance and optical absorption studies of irradiated phosphorus-doped silica glass and optical fibers," *J. Appl. Phys.*, vol. 54, no. 7, pp. 3743–3762, Jul. 1983.
- [22] D. Di Francesca et al., "Combined temperature radiation effects and influence of drawing conditions on phosphorous-doped optical fibers," *Phys. Status Solidi A*, vol. 216, no. 3, Dec. 2018, Art. no. 1800553.
- [23] G. Li Vecchi et al., "Infrared radiation induced attenuation of radiation sensitive optical fibers: Influence of temperature and modal propagation," *Opt. Fiber Technol.*, vol. 55, Mar. 2020, Art. no. 102166.